SCIENCE OF THE TOTAL ENVIRONMENT 407 (2009) 2306–2314

available at www.sciencedirect.com

ScienceDirect

www.elsevier.com/locate/scitotenv

Temporal and spatial distributions of total gaseous mercury concentrations in ambient air in a mountainous area in southwestern China: Implications for industrial and domestic mercury emissions in remote areas in China

Xuewu Fu[a], *Xinbin Feng*[a,*], *Shaofeng Wang*[b], *S. Rothenberg*[a], *Lihai Shang*[a], *Zhonggen Li*[a], *Guangle Qiu*[a]

[a]*State Key Laboratory of Environmental Geochemistry, Institute of Geochemistry, Chinese Academy of Sciences, Guiyang 550002, PR China*
[b]*Key Laboratory of Terrestrial Ecological Process, Institute of Applied Ecology, Chinese Academy of Sciences, Shenyang, China*

ARTICLE DATA

Article history:
Received 23 August 2008
Received in revised form
20 November 2008
Accepted 21 November 2008
Available online 12 January 2009

Keywords:
Total gaseous mercury (TGM)
Temporal and spatial distribution
Smelting activities
Domestic Hg emission
Southwestern China

ABSTRACT

Spatial and temporal distributions of total gaseous mercury (TGM) concentrations in ambient air were investigated in the Mt. Gongga area (Sichuan province, PR China) from April 2006 to June 2007. The annual geometric mean TGM concentration at the Moxi baseline station was 3.90±1.20 ng m^{-3}. Geometric mean TGM concentrations at 14 representative sampling sites during the warm season ranged from 1.60 to 20.1 ng m^{-3} and varied spatially, with levels decreasing between urbanized areas and more remote regions: urban area (U1–U3: 7.76±4.57 to 20.1±15.1 ng m^{-3}), town (T1: 4.61±1.15 ng m^{-3}) and village (V1–V4: 3.26±0.63 to 8.45±3.06 ng m^{-3}), and remote area (R1–R6: 1.60±0.43 to 3.41±1.26 ng m^{-3}). Our study suggested that industrial activities, especially non-ferrous smelting activities, were an important source of atmospheric Hg and played a vital role in the regional distribution of TGM. In addition, domestic coal and biomass combustion to heat residential homes were important sources of TGM in densely populated areas during the winter months.

1. Introduction

Mercury (Hg) can be transported and transformed in the atmosphere, thus making this pathway particularly important in the Hg cycle (Lindqvist et al., 1991; Schroeder, 1996). Because of its high volatility, low chemical activity, and low solubility in water, Hg^0 (which is >95% of TGM) persists in the atmosphere about 0.5–2 years and is transported far beyond the region where it is emitted (Schroeder and Munthe, 1998). Recent studies have shown that long-range transport and deposition is the primary input pathway for Hg in pristine aquatic ecosystems (Meili, 1991; Lindqvist et al., 1991). In sites located far from anthropogenic sources, Hg is efficiently bioaccumulated in the aquatic food web, and consumption of contaminated fish has attracted global attention (Watras and Frost, 1989; Verta, 1996; Lindqvist et al., 1991; Rask and Metsala, 1991).

Atmospheric Hg emissions are increasing more quickly in China, compared to other regions in the world. Industrial coal burning together with non-ferrous smelting are the two primary emission sectors, which contribute about 80% of total Hg emissions in China (500–700 tons, Street et al., 2005). These two emission sources are likely responsible for increased atmospheric Hg concentrations in industrial zones and surrounding areas. Additionally, Hg emissions from domestic activities, including coal combustion, biomass burning, motor vehicles, and agriculture waste burning, are prevalent in China, and are likely responsible for elevated Hg

* *Corresponding author*. Tel.: +86 851 5891356; fax: +86 851 5891609.
E-mail address: fengxinbin@vip.skleg.cn (X. Feng).

0048-9697/$ – see front matter © 2008 Elsevier B.V. All rights reserved.
doi:10.1016/j.scitotenv.2008.11.053

Table 1 – TGM concentrations in ambient air reported in China

Locations	Classification	Sampling duration	Sampling techniques	TGM (ng m^{-3})	Reference
Guiyang	Urban	1 year	Tekran 2537 A	8.40	Feng et al., 2004a
Beijing	Urban	44 days	Tekran 2537A	6.2–16.7	Liu et al., 2002
Chongqing	Urban	1 year	RA-915$^+$	8.5	Wang et al., 2007a,b
Taiwan	Urban	9 months	Gardis-3	6.3–9.4	Kuo et al., 2005
Changchun	Urban	1 year	Tekran 2537 A	18.4	Fang et al., 2004
Changchun	Suburban	1 year	Tekran 2537 A	11.7	Fang et al., 2004
Guangzhou	Urban	2 weeks in Dec	RA-915$^+$	5.4	Wang et al., 2007a,b
Beijing	Rural	9 days	Tekran 2537 A	3.0–4.4	Liu et al., 2002
Taiwan	Rural	3 months	Gardis-3	6.1	Kuo et al., 2005
Baihua reservoir,	Rural	1 week in Nov	Tekran 2537 A	7.5	Feng et al., 2004b
Guizou provice		2 weeks in Apr	Tekran 2537 A	5.9	
Hongfeng lake,	Rural	5 days in Jul	Tekran 2537A	2.7	Feng et al., 2008
Guizou provice		4 days in March	Tekran 2537A	7.7	
Mt. Changbai	Rural	1 year	Tekran 2537A	3.58	Wan et al., in press

concentrations in many areas (Liu et al., 2002; Feng et al., 2004a; Fu et al., 2008a,b; Street et al., 2005). Table 1 summarizes atmospheric TGM levels measured in some areas in China, and it is clear that TGM concentrations in both urban and remote areas in China are elevated compared to Europe and North America, suggesting that the large Hg emissions in China may be causing serious pollution problems.

Elevated Hg levels in China have attracted global attention, and some attempts have been made to predict the spatial and temporal distribution of atmospheric Hg in China (Dastoor and Larocque, 2004; Seigneur et al., 2004; Li et al., 2007). However, atmospheric Hg emission inventories in China are not well developed, and information concerning regional and local Hg sources and their influence on the distribution of atmospheric Hg is limited. Compared to TGM concentrations reported in China (Table 1), modeling results have underestimated TGM concentrations in ambient air in China, and therefore, more scientific observation data are needed to clarify the discrepancy between models and observed levels. Factors regulating the distribution of atmospheric Hg are very complicated in China, which results in complex regional and spatial distributions of atmospheric Hg. Therefore, China must present more scientific data and evaluate the factors influencing atmospheric Hg concentrations. In this study, comprehensive measurements of atmospheric TGM were conducted in Mt. Gongga area, Sichuan province, southwestern China. The main objective of this study was to investigate the spatial and temporal distributions of atmospheric TGM in a mountainous area in southwestern China, and to determine the influence of Hg emissions from industrial activities and domestic activities on Hg distributions in the ambient air.

2. Experimental

2.1. *Sampling locations*

The study area was located in Mt. Gongga area in Sichuan province, southwestern China. There are more than 40 mountain peaks greater than 6000 m in elevation, while the highest elevation is 7556 m. The wind system in this area is dominated by mountain and valley winds with monsoon conditions not being well developed. Fig. 1A and B show the frequency distributions of mountain wind and valley wind at the Moxi baseline station (1640 m) and the subalpine observation station (3000) from June 2005 to May 2007

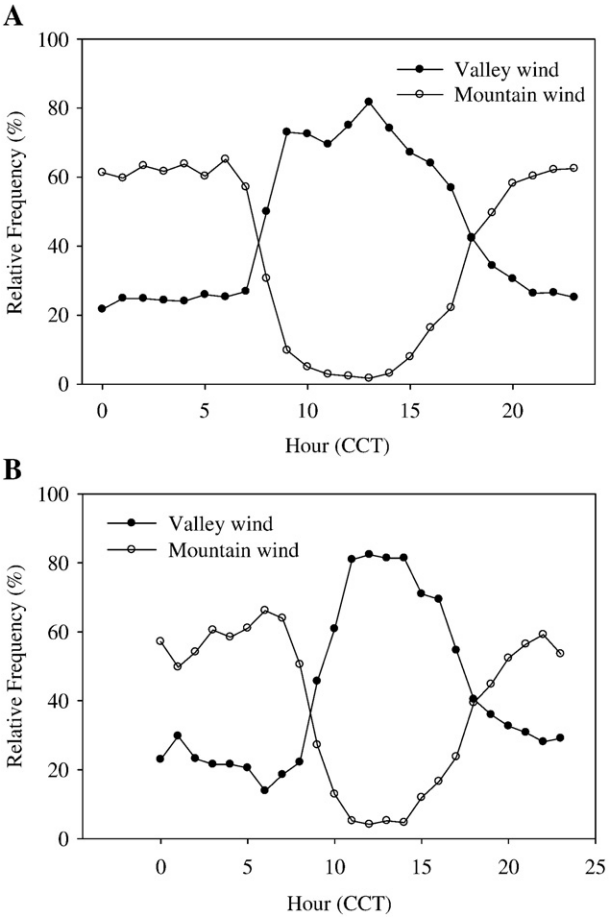

Fig. 1 – Relative frequency distributions of mountain wind and valley wind in Mt. Gongga area, A: Moxi baseline station (1640 m, valley wind direction: 90°–180°; mountain wind direction: 270°–360°); B: Subalpine observation station (3000 m, valley wind direction: 45° –135°; mountain wind direction: 225°–315°).

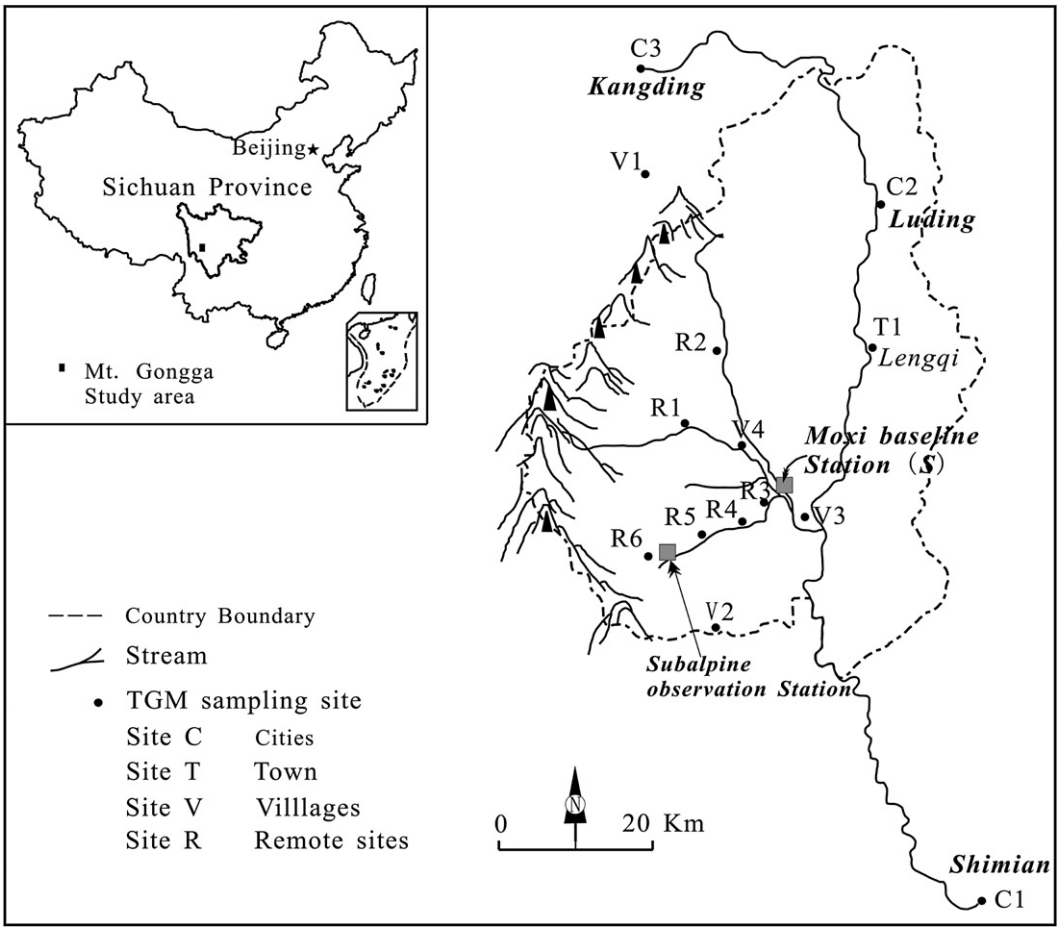

Fig. 2 – Locations of sampling sites in Mt. Gongga area.

(Fig. 2). It is clear that the mountain wind and valley wind dominate the total frequency (83.2% and 81.5%). In the daytime, the wind moves from lower to higher altitudes, while this trend is reversed at night. Since the study area is a mountainous area, we therefore supposed that mountain wind and valley wind dominated the winds at all sampling sites. The origin of air masses at all sampling sites in the daytime were from lower altitudes; while the air masses originated from mountain peaks and transported to lower altitudes during night. High spatial resolution measurements of ambient TGM were obtained at 15 sampling sites evenly dispersed across the Mt. Gongga area (Fig. 2), including one site (the Moxi baseline station), where TGM was monitored continuously for 1 year (June 2006 to May 2007). This station is located in the northwest region of Moxi town, and is equipped with standard metrological instrumentations for wind direction, wind speed, air temperature, solar radiation, and relative humidity (Fu et al., 2008a).

TGM levels were also monitored at 14 additional sampling sites from April 2006 to June 2007, using a sampling period of 2–4 days for each site. These 14 sampling sites were divided into the following four function zones:

(i) Urban area. U1 (102.35°E, 29.24°N, 921 m a.s.l.), U2 (102.23°E, 29.92°N, 1371 m a.s.l.), and U3 (101.97°E, 30.05°N, 2750 m a.s.l.) were located in Shimian, Luding, and Kangding cities, with populations of 32,000, 19,000, and 34,000, respectively. There is no large industrial activity in Luding and Kangding cities, although Shimian City is seriously polluted due to its proximity to a large industrial area with many non-ferrous smelting factories (3–4 km from valley wind direction).

(ii) Town. T1 was located in the town of Lengqi in the Dadu river valley, with a population of 8900.

(iii) Village. TGM measurements were monitored at 4 village sites (V1–V4), with populations between 200 and 1000. V1 was located 12 km south of Kangding city; V2 was located in Tianwan valley in mixed upland forest; V3 was located in the entrance of Moxi valley; and V4 was located 5 km northwest of Moxi town.

(iv) Remote area. Measurements were monitored at 6 remote sites (R1–R6) located far from anthropogenic activities. R1 and R2 were located in Yanzi and Yajiageng valleys, respectively. The other four remote sites (R3–R6) were located in Hailuogou valley. One site (R6, elevation=3100 m) was situated more than 32 km west of Moxi town.

Additionally, the spatial distribution of atmospheric TGM was studied during the cold season (Fig. 3). The sampling campaign was performed from 27 to 30 November, 2006, and 26 sampling sites were monitored to measure atmospheric

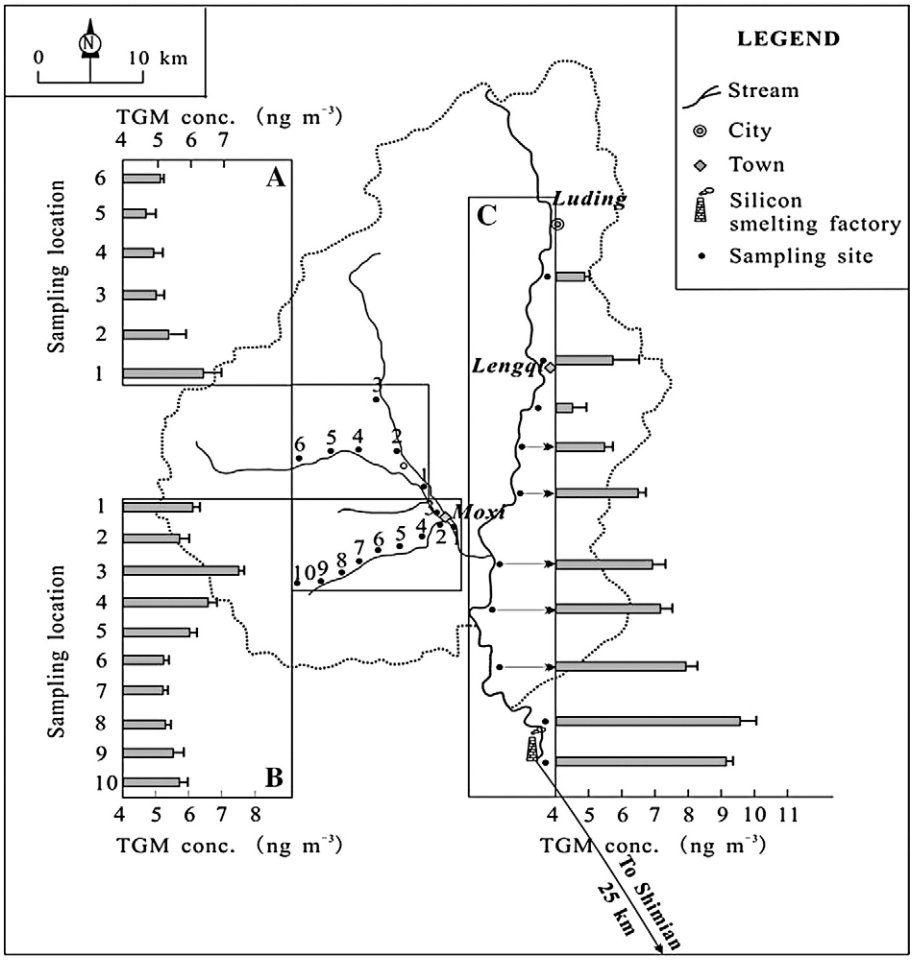

Fig. 3 – Locations and distributions of TGM concentrations in Mt. Gongga area in November 2006.

TGM. These measurements were monitored for a much shorter sampling period in the daytime (1 h per sampling site). In total, 10 TGM concentration data sets were collected, but only 7 data sets from behind the 10 data sets were used to calculate the mean TGM concentration at each site. The objective of this sampling campaign was to determine the effect of anthropogenic emissions, including industrial and residential coal use, on the regional distribution of TGM.

2.2. *TGM measurements*

A Tekran® 2537A Hg Vapor Analyzer (Tekran Inc. Toronto, Canada) was used to measure TGM concentrations in ambient air. Its technique is based on the collection of TGM on gold traps, followed by thermal desorption, and detection of Hg^0 by cold vapor atomic fluorescence spectrometry (λ=253.7 nm). The precision of Tekran Model 2537A is less than 2% and the detection limit is less than 0.1 ng m^{-3}. A heated (50 °C) sampling tube with its inlet 6 m above the ground was employed at the Moxi baseline station, while an acid-cleaned PTFE tube was used at the other sampling sites. The sampling flow rate was set at 1.0 L/min and 5.0 L air sample were collected during its 5-minute sampling intervals. During sampling, a 45 mm diameter Teflon filter (pore size 0.2 μm) was used to protect the sampling cartridges against contamination of airborne particulate matters. The data quality of Tekran Model 2537A was guaranteed via periodic internal recalibration with a 25 h interval and the internal permeation source was calibrated every 2 months (after the field measurement study, the external checks on the permeation source were within 97.4% (n=8) of expected values).

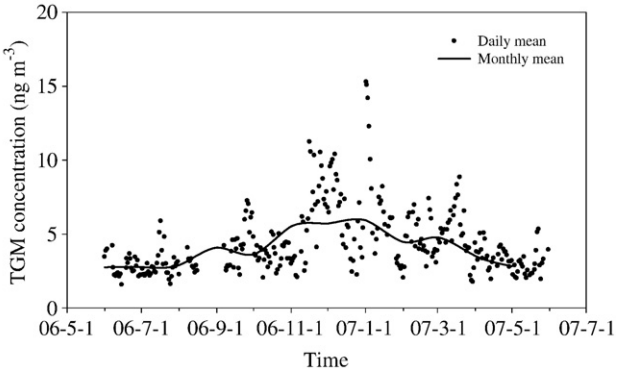

Fig. 4 – Daily and monthly distribution of TGM data sets at Moxi baseline station from June 2006 to May 2007.

3. Results

3.1. *Overall TGM distribution pattern at Moxi baseline station*

Temporal distribution of TGM in ambient air at Moxi baseline station from June 2006 to May 2007 is shown in Fig. 4. The annual geometric mean TGM concentration was 3.91±1.20 ng m^{-3} (Table 2), with higher concentrations during the cold season compared to the warm season. These results are consistent with previous annual data from the same location (3.98±1.16 ng m^{-3}, Fu et al., 2008a). Notable diurnal variations characterized by elevated concentrations during daytime were observed during the different seasons (Fig. 5). Largest diurnal variations were observed in spring (variation coefficients (CV=0.28)), followed by summer (CV=0.24), autumn (CV=0.24), and winter (CV=0.17). The geometric mean of TGM concentrations at the Moxi baseline station was slightly higher than the mean value observed at a remote sampling site located in the Changbai mountain area in northeastern China (3.22±1.78 ng m^{-3}, August 2005 to July 2006, Wan et al., in press), but it is much higher than the background values observed from remote areas in Europe and North America (~1.5–1.7 ng m^{-3}, Lindberg et al., 2007).

3.2. *Warm season spatial distributions of TGM*

A statistical summary of warm season TGM concentrations at 14 sampling sites is presented in Table 2, and it is clear there are large differences between urban and remote areas. The geometric mean TGM concentrations at the 14 sampling sites ranged from 1.60 to 20.1 ng m^{-3} and had a clear regional variation pattern: urban area (U1–U3: 7.76±4.57 to 20.1±15.1 ng m^{-3}), town (T1: 4.61±1.15 ng m^{-3}) and village (V1–V4: 3.26±0.63 to 8.45±3.06 ng m^{-3}), and remote area (R1–R6: 1.60±0.43 to 3.41±1.26 ng m^{-3}), which are listed in descending order.

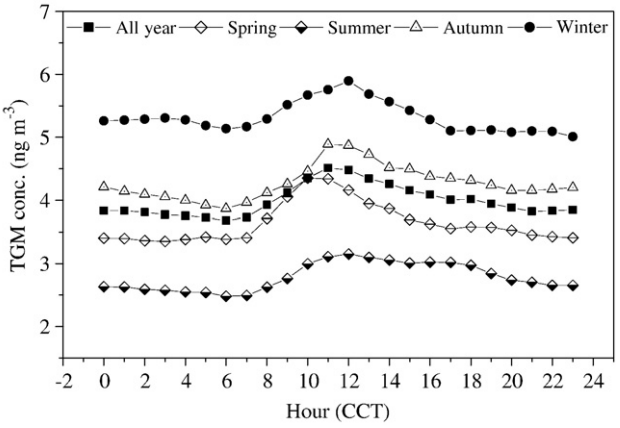

Fig. 5 – Diurnal variations of TGM concentrations in different seasons at Moxi baseline station.

The levels of TGM concentrations in these urban areas were much higher than those observed at other sampling sites in this region (Table 2), but they were comparable to previous data measured in Chinese cities (Table 1). For the three urban sampling sites, the highest geometric mean TGM concentration was obtained from Shimian city (Geometric mean: 22.53 ng m^{-3}). Shimian city is a famous industrial area in southwestern China, and mercury emissions from zinc smelting activities constitute the greatest source of atmospheric mercury. There were no industrial factories in Luding and Kangding cities, and the dominant mercury emission sources in these two cities were domestic coal combustion and motor vehicles (Liu et al., 2002; Feng et al., 2004a; Landis et al., 2007). The mean TGM concentrations in Luding and Kangding cities were 7.76 and 8.82 ng m^{-3}, respectively, which were much lower than levels observed in Shimian city.

Table 2 – Statistical summary of TGM concentrations at 15 sampling sites in Mt. Gongga area

Site	Altitude (m)	Seasons	Start time	End time	Geometric mean	Std.	Variation coefficient	Median	Min	Max	N
S	1640	All year	06-6-1	07-5-31	3.91	1.20	0.31	3.85	0.90	43.7	72811
		Summer	06-6-1	06-8-31	2.80	0.93	0.33	2.70	1.01	9.10	15037
		Autumn	06-9-1	06-11-30	4.34	2.36	0.54	4.15	1.35	16.9	15818
		Winter	06-12-1	07-2-28	5.33	2.98	0.56	5.30	1.08	39.4	20857
		Spring	07-3-1	07-5-31	3.62	1.66	0.46	3.66	0.90	43.7	21099
U1	921	Spring	07-5-28	07-5-30	20.1	15.1	0.75	19.5	8.23	222	548
U2	1371	Summer	07-6-1	07-6-3	7.76	4.57	0.59	6.59	3.82	33.0	559
U3	2750	Summer	07-6-3	07-6-5	8.82	2.15	0.24	8.66	5.30	19.9	528
T1*	1280	Autumn	06-9-2	06-9-4	4.61	1.15	0.25	4.51	3.09	9.39	282
V1	2920	Summer	07-6-5	07-6-7	8.45	3.06	0.36	8.76	5.82	23.7	581
V2*	1220	Summer	06-8-27	06-8-29	3.60	0.50	0.14	3.68	2.58	4.68	270
V3*	1300	Autumn	06-9-4	06-9-6	3.34	0.50	0.15	3.29	2.09	4.85	314
V4*	1900	Summer	06-8-22	06-8-27	3.26	0.63	0.19	3.24	2.01	5.00	634
R1*	2350	Summer	06-8-21	06-8-22	3.41	1.26	0.37	3.22	2.36	8.54	132
R2	2200	Spring	06-4-11	06-4-13	2.29	0.39	0.17	2.24	1.59	3.75	462
R3*	1650	Summer	06-8-17	06-8-18	2.38	0.43	0.18	2.36	1.36	3.66	180
R4*	2140	Summer	06-8-19	06-8-21	2.27	0.30	0.13	2.29	1.34	3.04	276
R5*	250	Summer	06-8-30	06-8-31	2.00	0.63	0.32	1.96	0.74	3.48	160
R6*	3050	Summer	06-8-31	06-9-1	1.60	0.43	0.27	1.66	0.94	2.52	134

*10-minute sampling intervals.

TGM concentrations in ambient air in the urban areas in Mt. Gongga area were much higher compared to cities in other countries, including Seoul, Korea (5.26 ng m^{-3}, Kim and Kim, 2001), Tokyo, Japan (3.5±1.4 ng m^{-3}, Sakata and Marumoto, 2002), Reno, Nevada, USA (2.3 ng m^{-3}, Stamenkovic et al., 2007), Chicago, USA (3.6±2.9 ng m^{-3}, Landis et al., 2002), Detroit, Michigan, USA (1.69–3.13 ng m^{-3}, Lynam and Keeler, 2005), Manhattan, New York, USA (3.3–4.56 ng m^{-3}, Carpi and Chen, 2002), Toronto, Canada (2.7 (1.0–7.4) ng m^{-3}, Eckley et al., 2008), and Grenoble, France (3.4 ng m^{-3}, Dommergue et al., 2007). Differences in energy sources, industrial structures, and control technologies may contribute to the great difference in atmospheric TGM concentrations between cities in China and cities elsewhere.

No distinction in TGM concentrations was observed between the town and villages; the geometric mean TGM concentration at Lengqi town was 4.41±1.15 ng m^{-3}, which was comparable to those observed from other villages. Except for the sampling site V1, the geometric mean of TGM concentrations at the other three village sites fell between 3 and 4 ng m^{-3}, which were much lower than levels observed in urban areas, indicating those villages were less impacted by human activities. However, the geometric mean TGM concentration at V1 reached 8.84 ng m^{-3} and was 2–3 times higher than those from the other three village sampling sites. Elevated TGM levels at V1 may be due to its location 12 km valley-wind from Kangding city, where higher TGM levels were observed (TGM mean: 9.04±2.15 ng m^{-3}) and may be efficiently transported through the valley to V1.

Geometric mean TGM concentrations at six remote sampling sites were much lower than those observed from other functional zones, possibly because these sampling sites were located far from residential areas and therefore less affected by anthropogenic Hg emissions. TGM concentrations showed a clear decreasing trend while going up the mountain peak. The lowest geometric mean of TGM was observed at R6, which

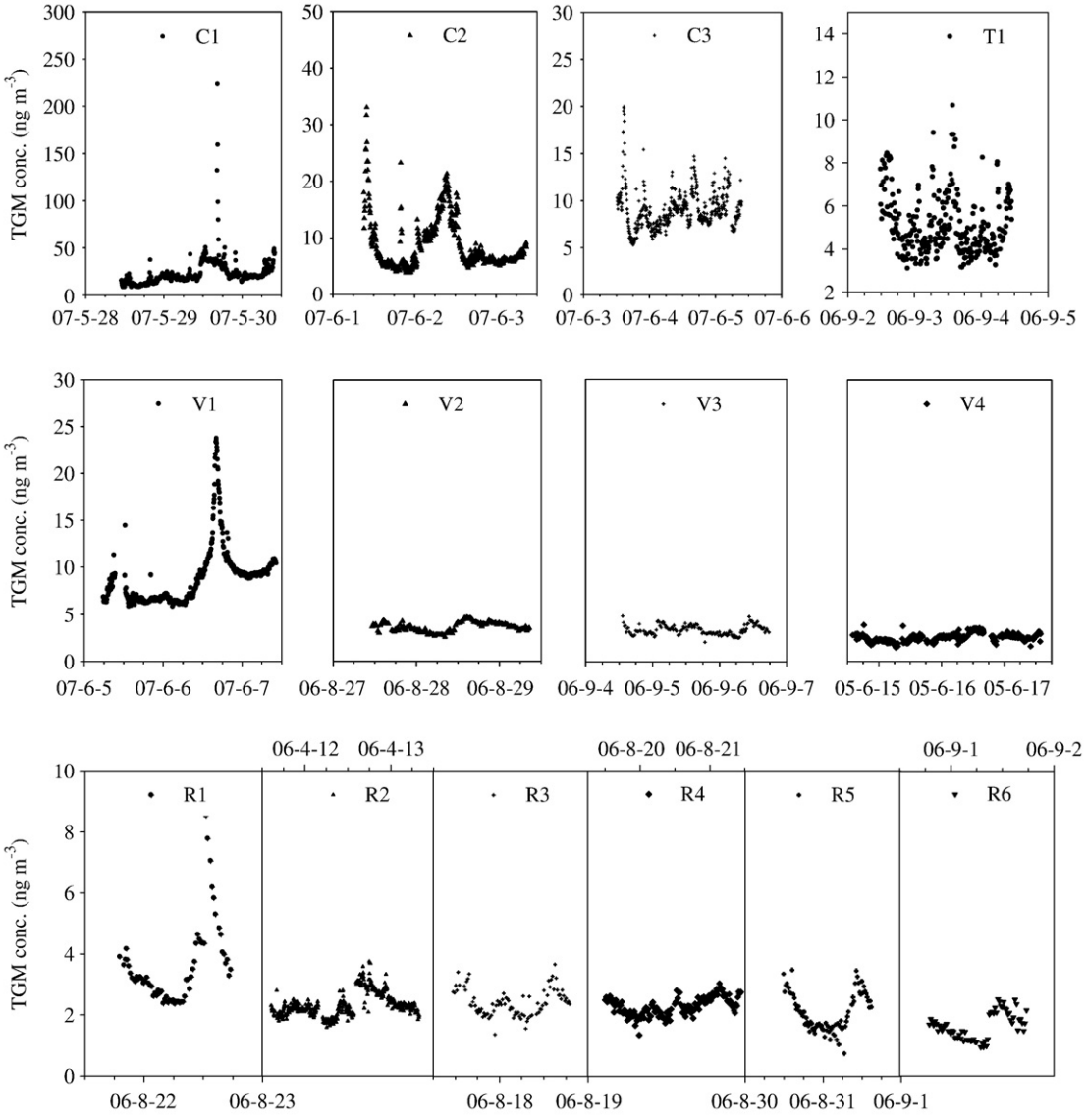

Fig. 6 – Time series of total gaseous mercury (TGM) concentrations at 14 monitoring sites in Mt. Gongga area in warm season (5 or 10 minute intervals).

was located more than 30 km from the residential area. Aside from sampling site R6, TGM concentrations at the other 5 remote sampling sites were much higher than the values observed in the background areas in Europe and North America, implying that regional background TGM concentrations in the ambient air were elevated.

3.3. *Variation of TGM concentrations in cold season*

Fig. 3 shows the cold season spatial variation of TGM concentrations in Mt. Gongga area. Cold season TGM concentrations were elevated compared to the warm season measurements at corresponding or nearby sampling sites and averaged 2.39 (range: 1.28–3.53 ng m^{-3}). This trend was similar to seasonal variations observed at the Moxi baseline station. Generally, higher elevated levels of TGM concentrations during the cold season were observed at higher elevations, which might be attributed to the higher frequency of the temperature inversion layer during the cold season.

Large uncertainties are associated with these observations due to short-term sampling periods, which do not accurately reflect TGM levels at each sampling sites. However, three notable profiles of TGM concentrations were observed as shown in Fig. 3. First, TGM concentrations clearly decreased from the sites close to Shimian city to the sites further away (Fig. 3C). In the second and third profiles (Fig. 3A and B), TGM concentrations decreased fast while going up to mountain peaks far from anthropogenic activities (the coefficients of variation (CV) for TGM concentrations in profiles A and B were 0.59 and 0.40, respectively, which were much higher than the diurnal CV at Moxi baseline station in winter, 0.17, indicating the spatial variations of TGM and not being influenced by temporal changes). These profiles indicate that Hg emissions from anthropogenic activities played a vital role in the distribution of TGM.

4. Discussion

Fig. 6 represents the high-temporal resolved data sets of TGM concentrations at 14 sampling sites during the warm season, and it is clear that considerable variability in TGM levels was observed at most of the sampling sites. Of the 14 sampling sites, the geometric mean concentration and data variability of TGM at U1 site (CV: 0.75) were both much higher compared to other sites, which indicated impacts from nearby Hg emission sources. Recent inventories of Hg emissions from anthropogenic sources in China confirmed that non-ferrous smelting activities (especially Zn production) are becoming one of the largest emission sources in China (Street et al., 2005). The elevated TGM concentrations at U1 may result from several Zn smelting factories (annual Zn production: 5 tons) located in the valley wind direction of the sampling site.

Domestic coal and biomass combustion was an additional atmospheric TGM source in the study area. Coal and biomass combustion for residential use are important Hg sources in China, contributing more than 30 tons of Hg in China (Street et al., 2005; Friedli et al., 2003). The domestic consumption of coal and biomass were very high in the study area. For example, the annual consumption of coal and biomass in Moxi town (population ~7000) was about 900 and 500 tons, respectively. Using the average emission factors for domestic coal and biomass combustion (0.5 and 0.02 g/ton, from Street et al., 2005; Pacyna et al., 2006), the annual Hg emission from domestic coal and biomass combustion in Moxi town reached 460 g. Aside from U1, there was no industrial activity in Mt. Gongga area; therefore, Hg emissions from domestic coal and biomass combustion were important sources at sampling sites near residential areas. U2, U3, T1, and V2 were all located within residential areas, and these sites received more Hg emissions from domestic coal and biomass combustion and showed higher TGM concentrations. Diurnal distribution patterns with high TGM concentrations during the daytime were observed at most of the sampling sites (Fig. 6), which may be due to the alternation of mountain wind and valley wind and residential activities. During the day, valley wind from Shimian city and residential areas carried polluted Hg air to the sampling sites (Fu et al., 2008a). Additionally, during the cold season, more coal and biomass were consumed for residential heating, and this would result in elevated TGM concentrations during the day. The U2 site was located in a residential area in the Luding city, in which there was no industrial activity and the dominant atmospheric Hg source was likely the domestic activity. Elevated daytime TGM concentrations at U2 were possibly due to enhanced domestic activities, including coal and biomass burning. Increased TGM concentrations were observed for areas located downwind and upwind of Moxi town (wind direction: 142°) and Lengqi town (wind direction: 192°), which were 1.97 and 1.96 ng m^{-3}, respectively. The increase in TGM concentration accounted for 25% of the average TGM concentration at Moxi monitoring site, and this may be attributed to Hg emissions from house heating activities.

For the remote monitoring sites, the regional transport of TGM in ambient air played an important role in the distribution of TGM. As shown in Fig. 3C, TGM concentrations were higher in sites close to Shimian city. This indicated Hg emissions from non-ferrous smelting activities in Shimian area were an important source of regional atmospheric TGM. Additionally, Hg emissions from domestic activities were another important source and could cause elevated TGM concentrations nearby, as observed at the V1 monitoring site. Since the surface winds were dominated by the mountain wind and valley wind system, the daytime air mass was from a lower altitude area, and likely transported higher levels of TGM (from non-ferrous smelting and domestic activities), causing diurnal variations in TGM at the remote sampling sites as shown in Fig. 6.

5. Conclusion

This study presents spatial and temporal variations of ambient air TGM concentrations in the Mt. Gongga area. TGM concentrations at Moxi monitoring site varied between 0.90 and 43.7 ng m^{-3}. The geometric mean concentration observation in 1 year was 3.91 ± 1.20 ng m^{-3}, which was much higher than values observed at remote sites in Europe and North America (1.5 to 2.0 ng m^{-3}, Lindberg et al., 2007). Geometric mean TGM concentrations at 14 representative

sampling sites in this area in the warm season (April–September) ranged across an order of magnitude from 1.60 to 20.1 ng m^{-3} and varied spatially: urban area (U1–U3: 7.76±4.57 to 20.1±15.1 ng m^{-3}), town (T1: 4.61±1.15 ng m^{-3}) and village (V1–V4: 3.26±0.63 to 8.45±3.06 ng m^{-3}), and remote area (R1–R6: 1.60±0.43 to 3.41±1.26 ng m^{-3}), listed in a descending order. Seasonal variations of TGM concentrations were consistent at all sampling sites in this area with higher TGM concentrations during the cold season and lower concentrations during the warm season.

Atmospheric TGM concentrations showed clear profiles, including high TGM concentrations near Shimian city and residential areas, and low TGM concentrations at more remote sites. Emissions of Hg from non-ferrous smelting activities in Shimian area not only caused serious pollution problem of atmospheric TGM in Shimian city, but also acted as an important source for other sampling sites. Domestic coal and biomass combustion was another emission source of atmospheric TGM in the study area, especially within densely populated areas. During the cold season, coal and biomass consumption increased, which contributed significantly to the high TGM levels.

Acknowledgments

This research was financially supported by the Chinese Academy of Sciences through an Innovation Foundation Award (KZCX3-SW-443), with additional support from the International Partnership Project, the Field Station Foundation, and the Natural Science Foundation of China (40532014). The authors would like to thank Mr. Li Wei, Mrs. Chen Binru for their sampling assistance. Finally, the authors thank the Institute of Mountain Hazards and Environment, CAS, for providing meteorological data.

REFERENCES

Carpi A, Chen YF. Gaseous elemental mercury fluxes in New York City. Water Air Soil Pollut 2002;140:371–9.

Dastoor AP, Larocque Y. Global circulation of atmospheric mercury: a modeling study. Atmos Environ 2004;38:147–61.

Dommergue A, Ferrrari CP, Planchon AM, Boutron CF. Influence of anthropogenic sources on total gaseous mercury variability in grenoble suburban air (France). Sci Total Environ 2007;297:203–13.

Eckley CS, Branfireun B, Diamond M, Van Metre P, Heitmuller F. Atmospheric mercury accumulation and washoff processes on impervious urban surfaces. Atmos Environ 2008;42:7429–38.

Fang FM, Wang QC, Li JF. Urban environmental mercury in Changchun, a metropolitan city in Northeastern China: source, cycle, and fate. Sci Total Environ 2004;330:159–70.

Feng XB, Tang SL, Shang LH, Yan HY, Zheng W. Temporal variation of total gaseous mercury in the air of Guiyang, China. J Geophy Res 2004(a);109:D03303. doi:10.1029/2003JD004159.

Feng XB, Yan HY, Wang SF, Qiu GL, Tang SL, Shang LH, et al. Seasonal variation of gaseous mercury exchange rate between air and water surface over Baihua Reservoir, Guizhou, China. Atmos Environ 2004(b);38:4721–32.

Feng XB, Wang SF, Qiu GL, He TR, Li GH, Li ZG, et al. Total gaseous mercury exchange between water and air during cloudy weather conditions over Hongfeng Reservoir, Guizhou, China. J Geophys Res 2008;113:D15309. doi:10.1029/2007JD009600.

Friedli HR, Radke LF, Lu JY, Banic CM, Leaitch WR, MacPherson JI. Mercury emissions from burning of biomass from temperate Northern American forests: Laboratory and airborne measurements. Atmos Environ 2003;37:253–67.

Fu XW, Feng XB, Zhu WZ, Wang SF, Lu J. Total gaseous mercury concentrations in ambient air in the eastern slope of Mt. Gongga, South-Eastern fringe of the Tibetan plateau, China. Atmos Environ 2008(a);42:70–979.

Fu XW, Feng XB, Zhu WZ, Zheng W, Wang SF, Lu JY. Total particulate and reactive gaseous mercury in ambient air on the eastern slope of the Mt.Gongga area, China. Appl Geochem 2008(b);23:408–18.

Kim KH, Kim MY. The temporal distribution characteristics of total gaseous mercury at an urban monitoring site in Seoul during 1999–2000. Atmos Environ 2001;35:4253–63.

Kuo TH, Chang TH, Urba A, Kvietkus K. Atmospheric gaseous mercury in Northern Taiwan. Sci Total Environ 2005;368:10–8.

Landis MS, Vette AF, Keeler GJ. Atmospheric mercury in the Lake Michigan basin: Influence of the Chicago/Gary urban area. Environ Sci Technol 2002;36:508–4517.

Landis MS, Lewis CW, Stevens RK, Keeler GJ, Dvonch JT, Tremblay RT. Ft. McHenry tunnel study: source profiles and mercury emissions from diesel and gasoline powered vehicles. Atmos Environ 2007;41:8711–24.

Li P, Chai TF, Carmichael GR, Tang YH, Street D, Woo TH, Friedli HR, et al. Top-down estimate of mercury emissions in China using four-dimensional variational data assimilation. Atmos Environ 2007;41:2804–19.

Lindberg SE, Bullock R, Ebinghaus R, Engstrom D, Feng XB, Fitzgerald W, et al. A synthesis of progress and uncertainties in attributing the sources of mercury in deposition. AMBIO 2007;36:19–32.

Lindqvist O, Johansson K, Bringmark L, Aastrup M, Timm B, Anderson A, et al. Mercury in the Swedish environment recent research on causes, consequences and corrective methods. Water Air Soil Pollut 1991;55:1–261.

Liu SL, Nadim F, Perkins C, Carley RJ, Hoag GE, Lin YH, et al. Atmospheric mercury monitoring survey in Beijing, China. Chemosphere 2002;48:97–107.

Lynam MM, Keeler GJ. Automated speciated mercury measurements in Michigan. Environ sci Technol 2005;39:9253–62.

Meili M. Fluxes, pools, and turnover of mercury in Swedish forest lakes. Water Air Soil Pollut 1991;56:19–727.

Pacyna EJ, Pacyna JM, Steenhuisen F, Wilson S. Global anthropogenic mercury emission inventory in 2000. Atmos Environ 2006;40:4048–63.

Rask M, Metsala R. Mercury concentrations in northern pike, *Esox Lucius* L in small lakes of Evo area, Southern Finland. Water Air Soil Pollut 1991;56:369–78.

Sakata M, Marumoto K. Formation of atmospheric particulate mercury in the Tokyo metropolitan area. Atmos Environ 2002;36:239.246.

Schroeder WH. Estimation of atmospheric input and evasion fluxes of mercury to and from the Great Lakes. In: Baeyens W, et al, editor. Global and Regional Mercury Cycles: Sources, Fluxes and Masse Balances; 1996. p. 109–21.

Schroeder WH, Munthe J. Atmospheric mercury: an overview. Atmos Environ 1998;32:809–22.

Stamenkovic J, Lynam S, Gustin MS. Seasonal and diel variation of atmospheric mercury concentrations in the Reno (Nevada, USA) airshed. Atmos Environ 2007;41:6662–72.

Seigneur C, Vijayaraghavan K, Lohman K, Karamchandani P, SCott C. Global source attribution for mercury deposition in the United States. Environ Sci Technol 2004;38:555–69.

Street DG, Hao JM, Wu Y, Jiang JK, Chan M, Tian HZ. Anthropogenic mercury emission in China. Atmos Environ 2005;39:7789–806.

Verta M. Mercury in Finnish forest lakes and reservoirs: anthropogenic contribution to the load and accumulation in fish. Publications of the Water and Environment Researchb Institute, vol. 6. National Board of Waters and the Environment, Finland; 1996.
Wan, Q., Feng, X.B., Lu, J.Y., Zheng, W., Song XJ, Han SJ, et al., in press. One year study for gaseous elementary mercury in Changbai Mountain area, Northwestern China. Environ Res.
Wang ZW, Chen ZS, Duan N, Zhang XS. Gaseous elemental mercury concentration in atmosphere at urban and remote sites in China. J Environ Sci 2007;19:176–80.
Wang PA, Zhang C, Wang CX, Wang DY. Research of spatial temporal variation of atmospheric mercury in Beibei District of Chongqing (in Chinese). J Southwest Univ 2007;29:125–9.
Watras CJ, Frost TM. Little rock lake: perspectives on an experimental approach to seepage lake acidification. Arch Environ Contam Toxicol 1989;18:157–65.